The Compact Muon Solenoid Experiment

CMS Note

Mailing address: CMS CERN, CH-1211 GENEVA 23, Switzerland

June 29, 2012

Searches for beyond-the-standard model physics in events with a Z boson, jets and missing transverse energy

D. Barge, C. Campagnari, D. Kovalskyi, V. Krutelyov

University of California, Santa Barbara, USA

W. Andrews, G. Cerati, D. Evans, F. Golf, I. MacNeill, S. Padhi, Y. Tu, F. Würthwein, A. Yagil, J. Yoo

University of California, San Diego, USA

L. Bauerdick, K. Burkett, I. Fisk, Y. Gao, O. Gutsche, B. Hooberman, S. Jindariani, J. Linacre, V. Martinez Outschoorn

Fermi National Accelerator Laboratory, Batavia, Illinois, USA

Abstract

This note describes a search for beyond-the-standard model (BSM) physics in events with a leptonically-decaying Z boson, jets, and missing transverse energy (E_T^{miss}). This signature is predicted to occur in several BSM scenarios, for example supersymmetric (SUSY) models. Two search strategies are pursued. The first is an inclusive approach which selects events with at least two jets and large E_T^{miss}, produced in association with the Z$\to \ell\ell$ candidate. The second is a targeted search in which additional requirements are imposed in order to achieve sensitivity to the production of the weakly-coupled SUSY charginos and neutralinos. The main backgrounds of SM $Z + $ jets and $t\bar{t}$ production are estimated with the data-driven E_T^{miss} templates technique and the opposite-flavor subtraction technique, respectively Additional backgrounds are estimated from simulation after validation in data control samples. No excesses above the SM expectations are observed. The results are interpreted in the context of simplified model spectra.

Contents

1 Introduction

This note presents two searches for beyond-the-standard model (BSM) physics in events containing a leptonically-decaying Z boson, jets, and missing transverse energy. This is an update of previous searches performed with 2011 data [1, 2]. The search is based on a data sample of pp collisions collected at $\sqrt{s} = 8$ TeV in 2012, corresponding to an integrated luminosity of 5.1 fb^{-1}.

The production of Z bosons is expected in many BSM scenarios, for example supersymmetric (SUSY) models. In SUSY models with neutralino lightest SUSY particle (LSP), Z bosons may be produced in the decays $\chi_2^0 \to Z\chi_1^0$, where χ_2^0 is the second lightest neutralino and χ_1^0 is the lightest neutralino. In models with gravitino LSP such as gauge-mediated SUSY breaking (GMSB) models, Z bosons may be produced via $\chi_1^0 \to Z\tilde{G}$, where $\tilde{G}$ is the gravitino. Such decays may occur either in the cascade decays of the strongly-produced squarks and gluinos, or via direct production of the electroweak charginos and neutralino. Examples of such processes (see Fig. 1) are:

- strong production: $pp \to \tilde{g}\tilde{g} \to (q\bar{q}\chi_2^0)(q\bar{q}\chi_2^0) \to (q\bar{q}Z\chi_1^0)(q\bar{q}Z\chi_1^0) \to ZZ + 4\text{ jets} + \text{E}_\text{T}^\text{miss}$

- electroweak production: $pp \to \chi_1^\pm \chi_2^0 \to (W\chi_1^0)(Z\chi_1^0) \to WZ + \text{E}_\text{T}^\text{miss}$
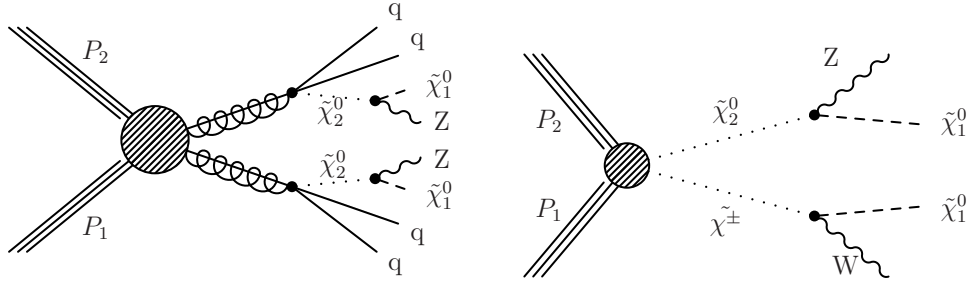

Figure 1: Examples of BSM physics signatures targeted in this search. In the left diagram, Z bosons are produced in the cascade decays of the strongly-interacting gluinos. In the right diagram, a Z boson is produced via direct production of the weakly-coupled charginos and neutralinos.

We thus pursue two strategies. The first is an inclusive strategy which selects events with a Z$\to \ell\ell$ candidate, at least two jets, and large E$_\text{T}^\text{miss}$. This strategy is useful for targeting, e.g., the production of Z bosons in the cascade decays of strongly-interacting particles as depicted in Fig. 1 (left). In the second strategy, we impose additional requirements which strongly suppress the backgrounds while retaining high efficiency for events with Z bosons produced via direct production of the weakly-coupled charginos and neutralinos. These two strategies are referred to as the "inclusive search" and the "targeted search," respectively.

After selecting events with jets and a Z$\to \ell^+\ell^-$ ($\ell = e, \mu$) candidate, the dominant background consists of SM Z production accompanied by jets from initial-state radiation ($Z + \text{jets}$). The E$_\text{T}^\text{miss}$ in $Z + \text{jets}$ events arises primarily when jet energies are mismeasured. The $Z + \text{jets}$ cross section is several orders of magnitude larger than our signal, and the artificial E$_\text{T}^\text{miss}$ is not necessarily well reproduced in simulation. Therefore, the critical prerequisite to a discovery of BSM physics in the $Z + \text{jets} + \text{E}_\text{T}^\text{miss}$ final state is to establish that a potential excess is not due to SM $Z + \text{jets}$ production accompanied by artificial E$_\text{T}^\text{miss}$ from jet mismeasurements. In this note, the $Z + \text{jets}$ background is estimated with the E$_\text{T}^\text{miss}$ templates technique, in which the artificial E$_\text{T}^\text{miss}$ in $Z + \text{jets}$ events is modeled using a $\gamma + \text{jets}$ control sample. The second background category consists of processes which produce leptons with uncorrelated flavor. These "flavor-symmetric" (FS) backgrounds, which are dominated by $t\bar{t}$ but also contain WW, DY$\to \tau\tau$ and single top processes, are estimated using a data control sample of eμ events. Additional backgrounds from WZ and ZZ production are estimated from MC, after validation of the MC modeling of these processes using 3-lepton and 4-lepton data control samples.

2 Datasets and Triggers

In this section we list the datasets, triggers, and MC samples used in the analysis. For selecting signal events, we use dilepton triggers in the DoubleElectron, DoubleMu, and MuEG datasets. An event in the ee final state is required to pass the dielectron trigger, a $\mu\mu$ event is required to pass the dimuon trigger, while an eμ event is required to pass at least one of the two $e - \mu$ cross triggers. The efficiencies of the ee, $\mu\mu$ and eμ triggers with respect to the offline selection have been measured as 0.95 ± 0.03, 0.88 ± 0.03, and 0.92 ± 0.03, respectively [6]. A sample of $\gamma + \mathrm{jets}$ events, used as a control sample to estimate the $Z + \mathrm{jets}$ background, is selected using a set of single photon triggers. The golden json of June 24th, corresponding to an integrated luminosity of 5.1 fb^{-1}, is used.

- Datasets

  - /DoubleElectron/Run2021A-PromptReco-v1/AOD
  - /DoubleMu/Run2021A-PromptReco-v1/AOD
  - /MuEG/Run2021A-PromptReco-v1/AOD
  - /DoubleElectron/Run2021B-PromptReco-v1/AOD
  - /DoubleMu/Run2021B-PromptReco-v1/AOD
  - /MuEG/Run2021B-PromptReco-v1/AOD

- Triggers

  - HLT_Mu17_Mu8_v*
  - HLT_Mu17_Ele8_CaloIdT_CaloIsoVL_TrkIdVL_TrkIsoVL_v*
  - HLT_Mu8_Ele17_CaloIdT_CaloIsoVL_TrkIdVL_TrkIsoVL*
  - HLT_Ele17_CaloIdT_CaloIsoVL_TrkIdVL_TrkIsoVL_Ele8_CaloIdT_CaloIsoVL_TrkIdVL_TrkIsoVL_v*
  - HLT_Photon22_R9Id90_HE10_Iso40_EBOnly_v*
  - HLT_Photon36_R9Id90_HE10_Iso40_EBOnly_v*
  - HLT_Photon50_R9Id90_HE10_Iso40_EBOnly_v*
  - HLT_Photon75_R9Id90_HE10_Iso40_EBOnly_v*
  - HLT_Photon90_R9Id90_HE10_Iso40_EBOnly_v*

- Good run list

  - Cert_190456-196531_8TeV_PromptReco_Collisions12_JSON.txt

- MC samples

  - /DYJetsToLL_M-50_TuneZ2Star_8TeV-madgraph-tarball/Summer12-PU_S7_START52_V9-v2
  - /TTJets_TuneZ2star_8TeV-madgraph-tauola/Summer12-PU_S7_START52_V9-v1
  - /WZJetsTo3LNu_TuneZ2_8TeV-madgraph-tauola/Summer12-PU_S7_START52_V9-v2
  - /WZJetsTo2L2Q_TuneZ2star_8TeV-madgraph-tauola/Summer12-PU_S7_START52_V9-v1
  - /ZZJetsTo2L2Q_TuneZ2star_8TeV-madgraph-tauola/Summer12-PU_S7_START52_V9-v3
  - /ZZJetsTo2L2Nu_TuneZ2star_8TeV-madgraph-tauola/Summer12-PU_S7_START52_V9-v3
  - /ZZJetsTo4L_TuneZ2star_8TeV-madgraph-tauola/Summer12-PU_S7_START52_V9-v3
  - /WWJetsTo2L2Nu_TuneZ2star_8TeV-madgraph-tauola/Summer12-PU_S7_START52_V9-v1
  - /T_tW-channel-DR_TuneZ2star_8TeV-powheg-tauola/Summer12-PU_S7_START52_V9-v1
  - /Tbar_tW-channel-DR_TuneZ2star_8TeV-powheg-tauola/Summer12-PU_S7_START52_V9-v1

3 Selection

In this section, we list the event selection, electron and muon objects selections, jets, E_T^{miss}, and b-tagging selections used in this analysis. These selections are based on those recommended by the relevant POG's.

3.1 Event Selection

We require the presence of at least one primary vertex satisfying the standard quality criteria; namely, vertex is not fake, $ndf \geq 4$, $\rho < 2$ cm, and $|z| < 24$ cm.

3.2 Lepton Selection

Because $Z \rightarrow \ell\ell$ ($\ell = e, \mu$) is a final state with very little background, we restrict ourselves to events in which the Z boson decays to electrons or muons only. Therefore opposite sign leptons passing the identification and isolation requirements described below are required in each event.

- $p_T > 20$ GeV and $|\eta| < 2.4$;

- Opposite-sign same-flavor (SF) ee and $\mu\mu$ lepton pairs (opposite-flavor (OF) eμ lepton pairs are retained in a control sample used to estimate the FS contribution);

- For SF events, the dilepton invariant mass is required to be consistent with the Z mass; namely $81 < m_{\ell\ell} < 101$ GeV.

3.2.1 Electron Selection

The electron selection is the loose working point recommended by the E/gamma POG, as documented at [3]. Electrons with $p_T > 20$ GeV and $|\eta| < 2.4$ are considered. We use PF-based isolation with a cone size of $\Delta R < 0.3$, using the effective area rho corrections documented at [4], and we require a relative isolation < 0.15. Electrons in the transition region defined by $1.4442 < |\eta_{SC}| < 1.566$ are rejected. The electron selection requirements are listed in Table 1 for completeness.

Table 1: Summary of the electron selection requirements.

Quantity	Barrel	Endcap
$\delta\eta$	< 0.007	< 0.009
$\delta\phi$	< 0.15	< 0.10
$\sigma_{i\eta i\eta}$	< 0.01	< 0.03
H/E	< 0.12	< 0.10
d_0 (w.r.t. 1st good PV)	< 0.02 cm	< 0.02 cm
d_z (w.r.t. 1st good PV)	< 0.2 cm	< 0.2 cm
$|1/E - 1/P|$	< 0.05 GeV^{-1}	< 0.05 GeV^{-1}
PF isolation / p_T	< 0.15	< 0.15
conversion rejection: fit probability	$< 10^{-6}$	$< 10^{-6}$
conversion rejection: missing hits	≤ 1	≤ 1

3.2.2 Muon Selection

We use the tight muon selection recommended by the muon POG, as documented at [5]. Muons with $p_T > 20$ GeV and $|\eta| < 2.4$ are considered. We use PF-based isolation with a cone size of $\Delta R < 0.3$, using the $\Delta\beta$ PU correction scheme, and we require a relative isolation of < 0.15. The muon selection requirements are listed in Table 2 for completeness.

3.2.3 PF Leptons

For consistency with pfmet, both electrons and muons are required to be reconstructed as PF electrons and PF muons, respectively, with $p_T > 20$ GeV. For defining the dilepton invariant mass, the 4-momenta of the PF leptons are used.

5

Table 2: Summary of the muons selection requirements.

Quantity	Requirement
muon type	global muon and PF muon
χ^2/ndf	< 10
muon chamber hits	≥ 1
matched stations	≥ 2
d_0 (w.r.t. 1st good PV)	< 0.02 cm
d_z (w.r.t. 1st good PV)	< 0.5 cm
pixel hits	≥ 1
tracker layers	≥ 5

3.3   Photons

As will be explained later, it is not essential that we select real photons. What is needed are jets that are predominantly electromagnetic, well measured in the ECAL, and hence less likely to contribute to fake MET. We select photons with:

- $p_T > 22$ GeV

- $|\eta| < 2$

- $H/E < 0.1$

- No matching pixel track (pixel veto)

- There must be a pfjet of $p_T > 10$ GeV matched to the photon within $dR < 0.3$. The matched jet is required to have a neutral electromagnetic energy fraction of at least 70%.

- We require that the pfjet p_T matched to the photon satisfy (pfjet p_T - photon p_T) > -5 GeV. This removes a few rare cases in which "overcleaning" of a pfjet generates fake MET.

- We also match photons to calojets and require (calojet p_T - photon p_T) > -5 GeV (the same requirement used for pfjets). This is to remove other rare cases in which fake energy is added to the photon object but not the calojet.

- We reject photons which have an electron of at least $p_T > 10$ GeV within $dR < 0.2$ in order to reject conversions from electrons from W decays which are accompanied by real MET.

- We reject photons which are aligned with the MET to within 0.14 radians in phi.

3.4   MET

We use pfmet, henceforth referred to simply as $\mathrm{E_T^{miss}}$.

3.5   Jets

- PF jets with L1FastL2L3 corrections (MC), L1FastL2L3residual corrections (data), using the 52X jet energy corrections

- $|\eta| < 2.5$

- Passes loose PFJet ID

- $p_T > 30$ GeV for determining the jet multiplicity, $p_T > 15$ GeV for calculation of H_T

- For the creation of photon templates, the jet matched to the photon passing the photon selection described above is vetoed

- For the dilepton sample, jets are vetoed if they are within $\Delta R < 0.4$ from any lepton $p_T > 20$ GeV passing analysis selection

6

4 Data vs. MC Comparison in Preselection Region

In this section we compare the data and MC samples passing the selection described in Sec. 3 In the following, the MC is reweighted to match the data distribution of number of reconstructed primary vertices. The trigger efficiencies of Sec. 2 are applied. In all plots, the last bin contains the overflow.

We begin by counting the inclusive Z yields. Here we require the presence of two selected leptons without any additional requirements on jets or E_T^{miss}. In Fig. 2 the distribution of dilepton invariant mass in the ee and $\mu\mu$ channels is displayed. In Table 3 the yields for selected dilepton events in the Z mass window are indicated. Good data vs. MC agreement is observed, within the systematic uncertainties of integrated luminosity (4.5%), trigger efficiency (3%), $Z + \mathrm{jets}$ and $t\bar{t}$ cross sections.
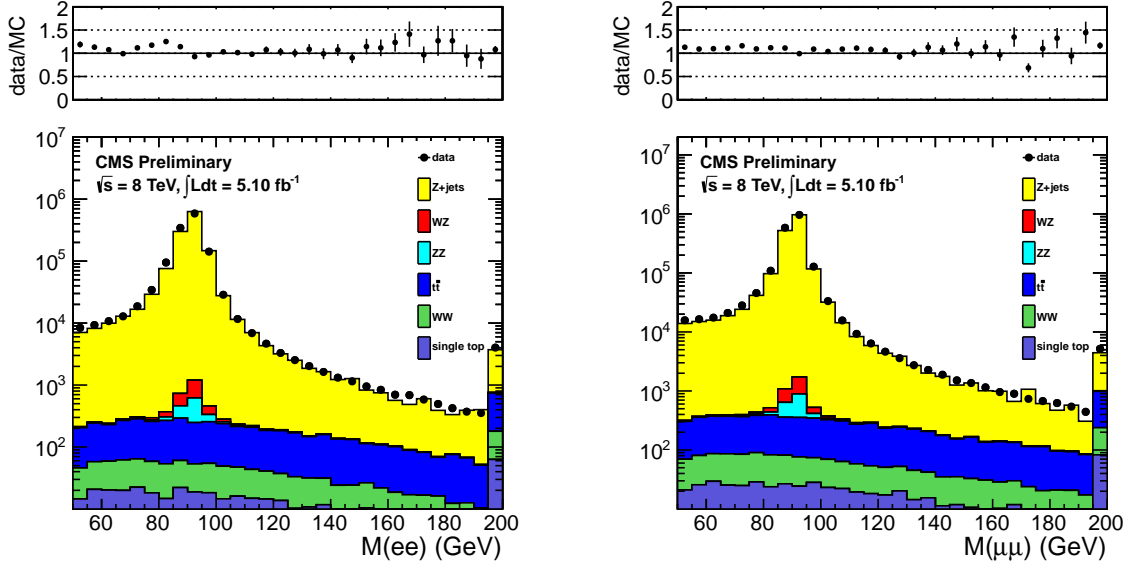

Figure 2: Dilepton mass distribution for events with two selected leptons in the ee (left) and $\mu\mu$ (right) final states.

Table 3: Data and Monte Carlo yields for events with two selected leptons in the Z mass window.

Sample	ee	$\mu\mu$	$e\mu$	total
$Z + \mathrm{jets}$	1150211.5 ± 4886.0	1697568.1 ± 5680.2	281.5 ± 63.7	2848061.2 ± 7492.8
$t\bar{t}$	829.1 ± 20.0	1120.7 ± 22.6	1910.9 ± 29.7	3860.7 ± 42.4
WZ	1038.2 ± 3.6	1465.5 ± 4.1	29.5 ± 0.5	2533.2 ± 5.5
ZZ	658.0 ± 2.4	933.0 ± 2.7	2.7 ± 0.1	1593.7 ± 3.6
WW	146.7 ± 2.6	209.0 ± 2.9	358.9 ± 3.9	714.6 ± 5.5
single top	70.9 ± 4.9	103.3 ± 5.7	172.5 ± 7.4	346.7 ± 10.5
total SM MC	1152954.5 ± 4886.1	1701399.6 ± 5680.3	2756.1 ± 70.8	2857110.2 ± 7493.0
data	1162229	1774353	3077	2939659

We next define the preselection region for the inclusive search using the following requirements:

- Number of jets ≥ 2;

- Same flavor dileptons (opposite flavor yields will be shown since they are used in data for the FS background estimation);

- Dilepton invariant mass $81 < m_{\ell\ell} < 101$ GeV.

The dilepton mass distributions in the preselection region of the inclusive search (without the dilepton mass requirement applied) for the ee and $\mu\mu$ final states are shown in Figure 3. In Table 4 the data and MC yields in the preselection region are indicated. Good data vs. MC agreement is observed.
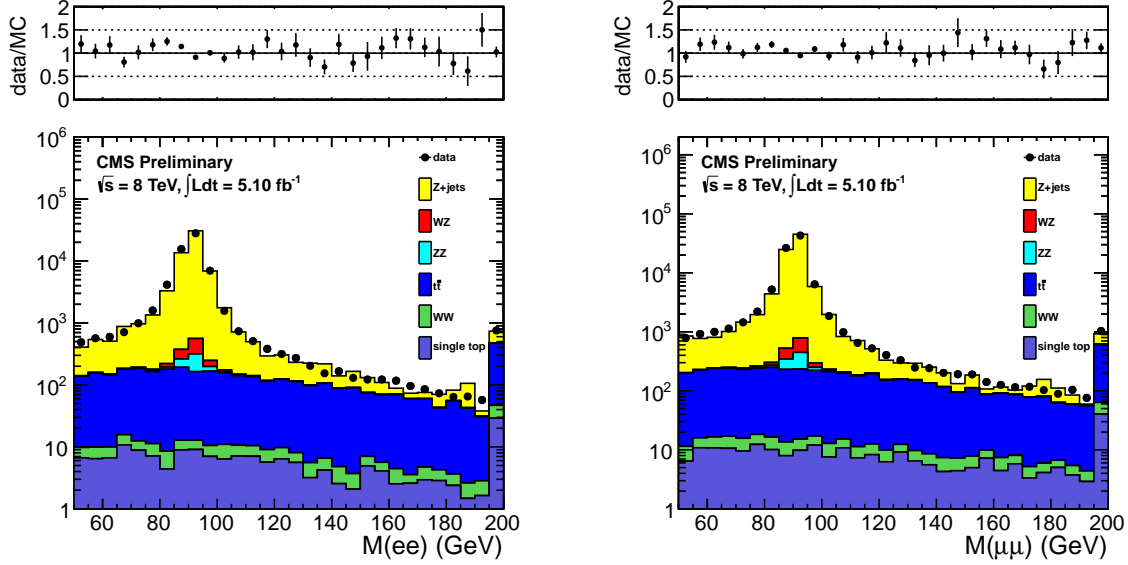

Figure 3: Dilepton mass distribution for events in the preselection region of the inclusive search in the ee (left) and $\mu\mu$ (right) final states.

Table 4: Data and MC yields in the preselection region of the inclusive search.

Sample	ee	$\mu\mu$	eμ	total
Z + jets	53187.8 ± 988.5	78070.5 ± 1165.7	5.6 ± 3.6	131264.0 ± 1528.4
$t\bar{t}$	645.3 ± 17.7	865.1 ± 19.7	1470.4 ± 25.8	2980.8 ± 37.0
WZ	431.2 ± 2.4	594.6 ± 2.7	5.8 ± 0.2	1031.6 ± 3.6
ZZ	269.9 ± 1.6	377.7 ± 1.8	0.5 ± 0.0	648.1 ± 2.4
WW	15.2 ± 0.8	22.2 ± 0.9	38.9 ± 1.3	76.4 ± 1.7
single top	28.8 ± 3.2	38.0 ± 3.4	72.0 ± 4.9	138.8 ± 6.7
total SM MC	54578.1 ± 988.7	79968.3 ± 1165.9	1593.3 ± 26.5	136139.7 ± 1528.9
data	54426	80367	1565	136358

We next define the preselection region for the targeted search by adding the following requirements:

- Veto events containing a b-tagged jet;

- Dijet invariant mass $70 < m_{jj} < 110$ GeV;

- Veto events containing a third selected lepton (electron or muon) with $p_T > 20$ GeV;

The rejection of events with a b-tagged jet strongly suppresses the $t\bar{t}$ background, which is the dominant background in the inclusive search after requiring large E_T^{miss}. The requirement that the jet pair is consistent with originating from W/Z decay is motivated by the fact that we are searching for signatures producing $V(jj)Z(\ell\ell)+E_T^{miss}$; this requirement suppresses the $Z + \text{jets}$ and $t\bar{t}$ backgrounds. The veto of events containing a third electron or muon suppresses the WZ background, and also serves to make this analyis exclusive with respect to searches in the trilepton final state.

The dilepton mass distributions in the preselection region of the targeted search (without the dilepton mass requirement applied) for the ee and $\mu\mu$ final states are shown in Figure 4. In Table 5 the data and MC yields in the preselection region are indicated. Good data vs. MC agreement is observed. We also show the distribution of dijet mass in the targeted preselection (with the requirement on this quantity removed) in Fig. 5, which demonstrates that the MC does a reasonable job of modeling this quantity.
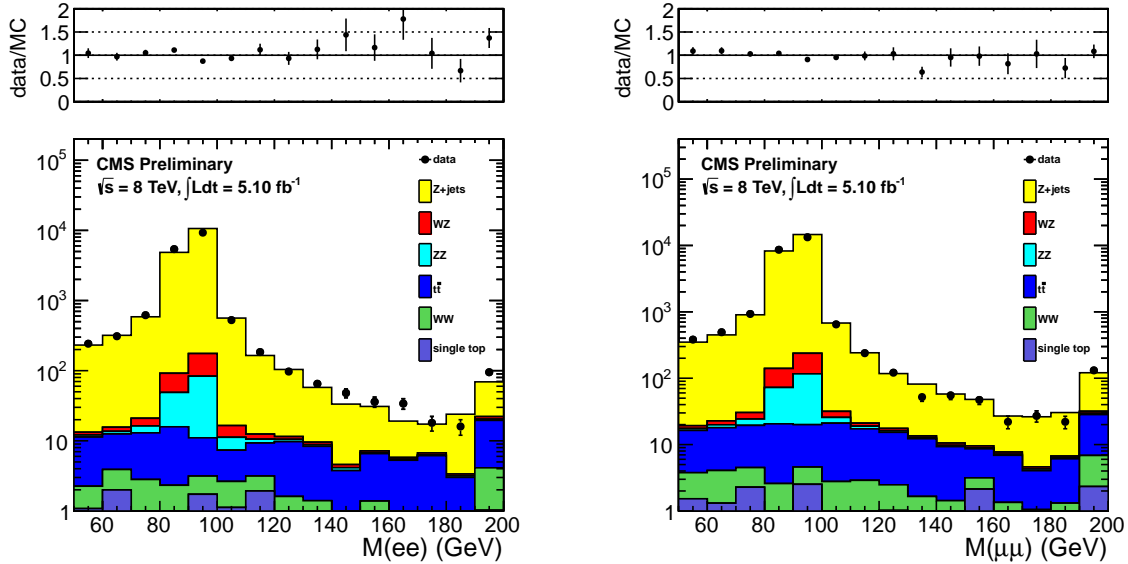

Figure 4: Dilepton mass distribution for events in the preselection region of the targeted search in the ee (left) and $\mu\mu$ (right) final states.

Table 5: Data and MC yields in the preselection region of the inclusive search.

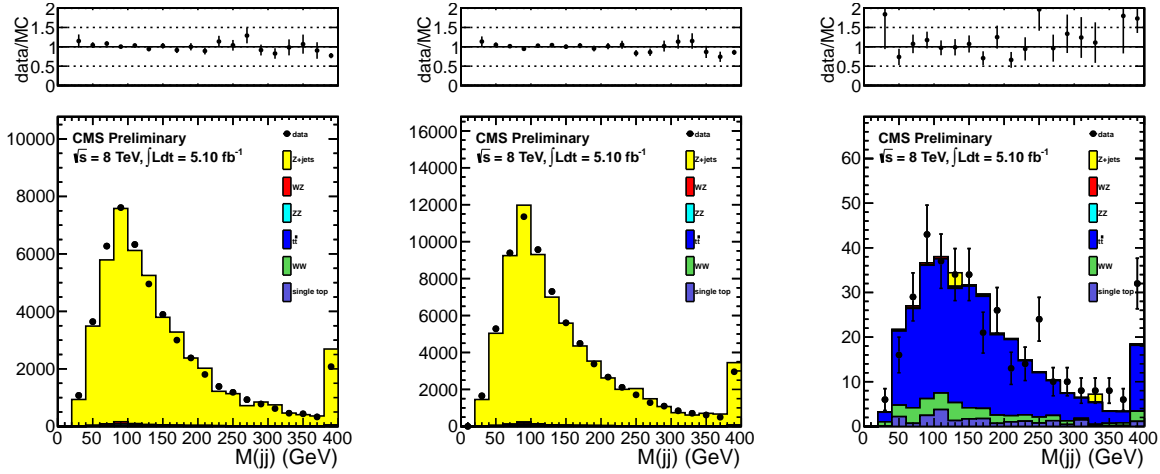| Sample	ee	$\mu\mu$	eμ	total
$Z + \text{jets}$	14108.9 ± 486.3	21927.1 ± 606.4	0.0 ± 0.0	36036.0 ± 777.4
$t\bar{t}$	21.0 ± 2.9	33.4 ± 3.9	53.7 ± 5.0	108.0 ± 6.9
WZ	135.6 ± 1.4	188.5 ± 1.6	1.0 ± 0.1	325.1 ± 2.1
ZZ	106.0 ± 1.0	148.8 ± 1.2	0.1 ± 0.0	254.9 ± 1.5
WW	3.4 ± 0.4	4.1 ± 0.4	7.8 ± 0.5	15.2 ± 0.7
single top	2.0 ± 0.8	2.8 ± 1.1	5.5 ± 1.4	10.3 ± 1.9
total SM MC	14376.9 ± 486.3	22304.7 ± 606.5	68.0 ± 5.2	36749.6 ± 777.4
data	14647	21840	74	36561

Figure 5: Distributions of dijet mass for the targeted preselection in the ee (left), $\mu\mu$ (middle) and eμ (right) final state.

5 Background Estimation Techniques

In this section we describe the techniques used to estimate the SM backgrounds in our signal regions defined by requirements of large E_T^{miss}. The SM backgrounds fall into three categories:

- $Z + \text{jets}$: this is the dominant background after the preselection. The E_T^{miss} in $Z + \text{jets}$ events is estimated with the "E_T^{miss} templates" technique described in Sec. 5.1;

- Flavor-symmetric (FS) backgrounds: this category includes processes which produces 2 leptons of uncorrelated flavor. It is dominated by $t\bar{t}$ but also contains $Z \rightarrow \tau\tau$, WW, and single top processes. This is the dominant contribution in the signal regions, and it is estimated using a data control sample of eμ events as described in Sec. 5.2;

- WZ and ZZ backgrounds: this background is estimated from MC, after validating the MC modeling of these processes using data control samples with jets and exactly 3 leptons (WZ control sample) and exactly 4 leptons (ZZ control sample) as described in Sec. 5.3;

5.1 Estimating the $Z + \text{jets}$ Background with E_T^{miss} Templates

The premise of this data driven technique is that E_T^{miss} in $Z + \text{jets}$ events is produced by the hadronic recoil system and *not* by the leptons making up the Z. Therefore, the basic idea of the E_T^{miss} template method is to measure the E_T^{miss} distribution in a control sample which has no true MET and the same general attributes regarding fake MET as in $Z + \text{jets}$ events. We thus use a sample of $\gamma + \text{jets}$ events, since both $Z + \text{jets}$ and $\gamma + \text{jets}$ events consist of a well-measured object recoiling against hadronic jets.

For selecting photon-like objects, the very loose photon selection described in Sec. 3.3 is used. It is not essential for the photon sample to have high purity. For our purposes, selecting jets with predominantly electromagnetic energy deposition in a good fiducial volume suffices to ensure that they are well measured and do not contribute to fake E_T^{miss}. The $\gamma + \text{jets}$ events are selected with a suite of single photon triggers with p_T thresholds varying from 22–90 GeV. The events are weighted by the trigger prescale such that $\gamma + \text{jets}$ events evenly sample the conditions over the full period of data taking. There remains a small difference in the PU conditions in the $\gamma + \text{jets}$ vs. $Z + \text{jets}$ samples due to the different dependencies of the γ vs. Z isolation efficiencies on PU. To account for this, we reweight the $\gamma + \text{jets}$ samples to match the distribution of reconstructed primary vertices in the $Z + \text{jets}$ sample.

To account for kinematic differences between the hadronic systems in the control vs. signal samples, we measure the E_T^{miss} distributions in the $\gamma + \text{jets}$ sample in bins of the number of jets and the scalar sum of jet transverse energies (H_T). These E_T^{miss} templates are extracted separately from the 5 single photon triggers with thresholds 22, 36, 50, 75, and 90 GeV, so that the templates are effectively binned in photon p_T . All E_T^{miss} distributions are

normalized to unit area to form "MET templates". The prediction of the MET in each Z event is the template which corresponds to the N_{jets}, H_T, and Z p_T in the $Z + \text{jets}$ event. The prediction for the Z sample is simply the sum of all such templates. All templates are displayed in App. B.

While there is in principle a small contribution from backgrounds other than $Z + \text{jets}$ in the preselection regions, this contribution is only $\approx 3\%$ ($\approx 2\%$) of the total sample in the inclusive search (targeted search), as shown in Table 4 (Table 5), and is therefore negligible compared to the total background uncertainty.

5.2 Estimating the Flavor-Symmetric Background with eμ Events

In this subsection we describe the background estimate for the FS background. Since this background produces equal rates of same-flavor (SF) ee and $\mu\mu$ lepton pairs as opposite-flavor (OF) eμ lepton pairs, the OF yield can be used to estimate the SF yield, after correcting for the different electron vs. muon offline selection efficiencies and the different efficiencies for the ee, $\mu\mu$, and eμ triggers.

An important quantity needed to translate from the OF yield to a prediction for the background in the SF final state is the ratio $R_{\mu e} = \epsilon_\mu / \epsilon_e$, where ϵ_μ (ϵ_e) indicates the offline muon (electron) selection efficiency. This quantity can be extracted from data using the observed Z$\to \mu\mu$ and Z$\to$ee yields in the preselection region, after correcting for the different trigger efficiencies.

Hence we define:

- $N_{ee}^{\text{trig}} = \epsilon_{ee}^{\text{trig}} N_{ee}^{\text{offline}}$,

- $N_{\mu\mu}^{\text{trig}} = \epsilon_{\mu\mu}^{\text{trig}} N_{\mu\mu}^{\text{offline}}$,

- $N_{e\mu}^{\text{trig}} = \epsilon_{e\mu}^{\text{trig}} N_{e\mu}^{\text{offline}}$.

Here $N_{\ell\ell}^{\text{trig}}$ denotes the number of selected Z events in the $\ell\ell$ channel passing the offline and trigger selection (in other words, the number of recorded and selected events), $\epsilon_{\ell\ell}^{\text{trig}}$ is the trigger efficiency, and $N_{\ell\ell}^{\text{offline}}$ is the number of events that would have passed the offline selection if the trigger had an efficiency of 100%. Thus we calculate the quantity:

$$R_{\mu e} = \sqrt{\frac{N_{\mu\mu}^{\text{offline}}}{N_{ee}^{\text{offline}}}} = \sqrt{\frac{N_{\mu\mu}^{\text{trig}}/\epsilon_{\mu\mu}^{\text{trig}}}{N_{ee}^{\text{trig}}/\epsilon_{ee}^{\text{trig}}}} = \sqrt{\frac{80367/0.88}{54426/0.95}} = 1.26 \pm 0.07. \tag{1}$$

Here we have used the Z$\to \mu\mu$ and Z$\to$ee yields from Table 4 and the trigger efficiencies quoted in Sec. 2. The indicated uncertainty is due to the 3% uncertainties in the trigger efficiencies. The predicted yields in the ee and $\mu\mu$ final states are calculated from the observed eμ yield as

- $N_{ee}^{\text{predicted}} = \frac{N_{e\mu}^{\text{trig}}}{\epsilon_{e\mu}^{\text{trig}}} \frac{\epsilon_{ee}^{\text{trig}}}{2R_{\mu e}} = \frac{N_{e\mu}^{\text{trig}}}{0.92} \frac{0.95}{2 \times 1.26} = (0.41 \pm 0.05) \times N_{e\mu}^{\text{trig}}$,

- $N_{\mu\mu}^{\text{predicted}} = \frac{N_{e\mu}^{\text{trig}}}{\epsilon_{e\mu}^{\text{trig}}} \frac{\epsilon_{\mu\mu}^{\text{trig}} R_{\mu e}}{2} = \frac{N_{e\mu}^{\text{trig}}}{0.95} \frac{0.88 \times 1.26}{2} = (0.58 \pm 0.07) \times N_{e\mu}^{\text{trig}}$,

and the predicted yield in the combined ee and $\mu\mu$ channel is simply the sum of these two predictions:

- $N_{ee+\mu\mu}^{\text{predicted}} = (0.99 \pm 0.06) \times N_{e\mu}^{\text{trig}}$.

Note that the relative uncertainty in the combined ee and $\mu\mu$ prediction is smaller than those for the individual ee and $\mu\mu$ predictions because the uncertainty in $R_{\mu e}$ cancels when summing the ee and $\mu\mu$ predictions.

To improve the statistical precision of the FS background estimate, we remove the requirement that the eμ lepton pair falls in the Z mass window. Instead we scale the eμ yield by K, the efficiency for eμ events to satisfy the Z mass requirement, extracted from simulation. In Fig. 6 we display the value of K in data and simulation, for a variety of E_T^{miss} requirements, for the inclusive analysis. Based on this we chose $K = 0.14 \pm 0.02$ for all E_T^{miss} regions except for $E_T^{\text{miss}} > 300$ GeV. For this region the statistical precision is reduced, so that we inflate the

11

231 uncertainty and chose $K = 0.14 \pm 0.08$. The corresponding plot for the targeted analysis, including the b-veto,
232 is displayed in Fig. 7. Based on this we chose $K = 0.13 \pm 0.02$ for all E_T^{miss} regions up to $E_T^{miss} > 100$ GeV.
233 For higher E_T^{miss} regions ($E_T^{miss} > 150$ GeV and above) the statistical precision is reduced, so that we inflate the
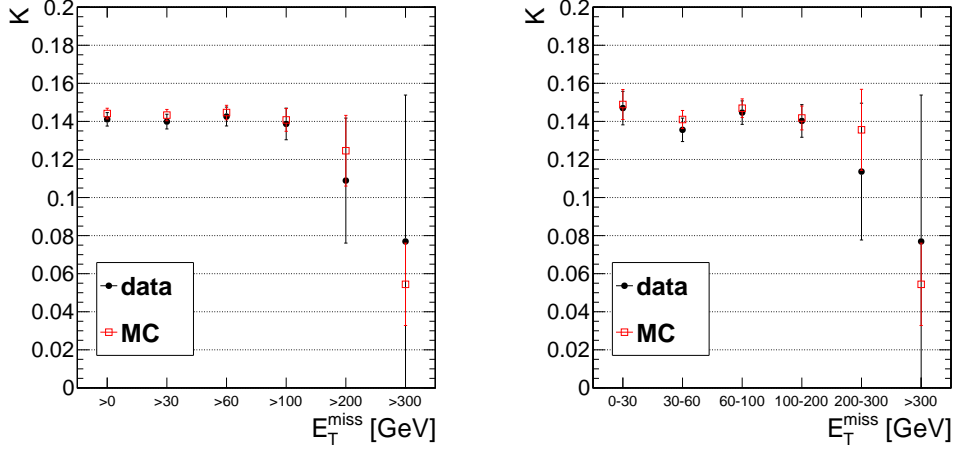234 uncertainty and chose $K = 0.13 \pm 0.07$.

Figure 6: The efficiency for $e\mu$ events to satisfy the dilepton mass requirement, K, in data and simulation for inclusive E_T^{miss} intervals (left) and exclusive E_T^{miss} intervals (right) for the inclusive analysis. Based on this we chose $K = 0.14 \pm 0.02$ for all E_T^{miss} regions except $E_T^{miss} > 300$ GeV, where we chose $K = 0.14 \pm 0.08$.
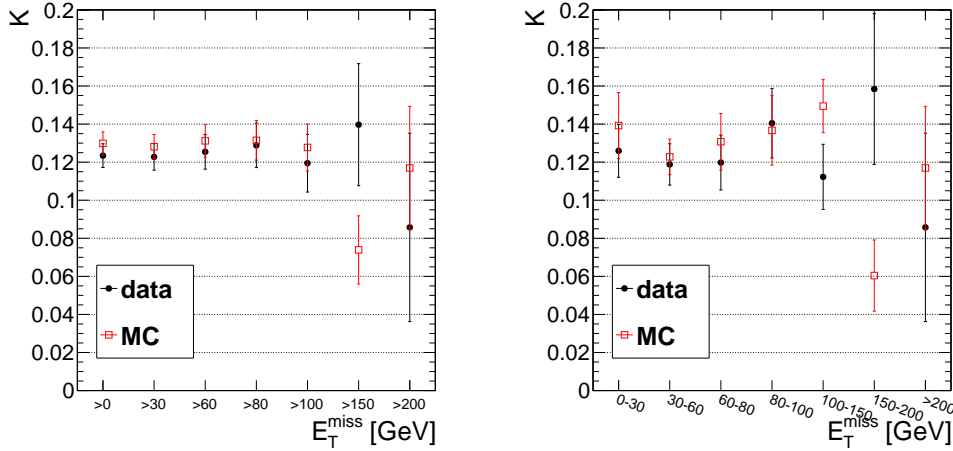

Figure 7: The efficiency for $e\mu$ events to satisfy the dilepton mass requirement, K, in data and simulation for inclusive E_T^{miss} intervals (left) and exclusive E_T^{miss} intervals (right) for the targeted analysis, including the b-veto. Based on this we chose $K = 0.13 \pm 0.02$ for the E_T^{miss} regions up to $E_T^{miss} > 100$ GeV. For higher E_T^{miss} regions we chose $K = 0.13 \pm 0.07$.

5.3 Estimating the WZ and ZZ Background with MC

Backgrounds from W($\ell\nu$)Z($\ell\ell$) where the W lepton is not identified or is outside acceptance, and Z($\nu\nu$)Z($\ell\ell$), are estimated from simulation. The MC modeling of these processes is validated by comparing the MC predictions with data in control samples with exactly 3 leptons (WZ control sample) and exactly 4 leptons (ZZ control sample). The relevant WZ and ZZ MC samples are:

- `/WZJetsTo3LNu_TuneZ2_8TeV-madgraph-tauola/Summer12-PU_S7_START52_V9-v2/AODSIM` ($\sigma = 1.058$ pb),

- `/ZZJetsTo4L_TuneZ2star_8TeV-madgraph-tauola/Summer12-PU_S7_START52_V9-v3/AODSIM` ($\sigma = 0.093$ pb),

The WZJetsTo2L2Q, ZZJetsTo2L2Q, and ZZJetsTo2L2Nu samples are also used in this analysis but their contribution to the 3-lepton and 4-lepton control samples is negligible.

5.3.1 WZ Validation Studies

A pure WZ sample can be selected in data with the requirements:

- Exactly 3 $p_T > 20$ GeV leptons passing analysis identication and isolation requirements,

- 2 of the 3 leptons must fall in the Z window 81-101 GeV,

- $E_T^{miss} > 50$ GeV (to suppress DY).

The data and MC yields passing the above selection are in Table 6. The inclusive yields (without any jet requirements) agree within 17%, which is approximately equal to the uncertainty in the measured WZ cross section. A data vs. MC comparison of kinematic distributions (jet multiplicity, E_T^{miss}, Z p_T) is given in Fig. 8. High E_T^{miss} values in WZ and ZZ events arise from highly boosted W or Z bosons that decay leptonically, and we therefore check that the MC does a reasonable job of reproducing the p_T distributions of the leptonically decaying Z. While the inclusive WZ yields are in reasonable agreement, we observe an excess in data in events with at least 2 jets, corresponding to the jet multiplicity requirement in our preselection. We observe 60 events in data while the MC predicts 34 ± 5.2 (stat), representing an excess of 78%, as indicated in Table 7. We note some possible contributions to this discrepancy:

- The $Z + \text{jets}$ contribution is under-estimated here, for 2 reasons: first, because the $Z + \text{jets}$ yield passing a $E_T^{miss} > 50$ GeV requirement is under-estimated in MC and second, because the fake rate is typically under-estimated in the MC. To get a rough idea for how much the excess depends on the $Z + \text{jets}$ yield, if the $Z + \text{jets}$ yield is doubled then the excess is reduced from 78% to 55%. Also note that we are currently using 10% of the $Z + \text{jets}$ MC sample and there is 1 event with a weight of about 5, so the plots and tables will be remade with full $Z + \text{jets}$ sample.

- The $t\bar{t}$ contribution is under-estimated here because the fake rate is typically under-estimated in the MC. To get a rough idea for how much the excess depends on the $t\bar{t}$ yield, if the $t\bar{t}$ yield is doubled then the excess is reduced from 78% to 57%.

- Currently no attempt is made to reject jets from pile-up interactions, which may be responsible for some of the excess at large N_{jets}. To check this, we increase the jet p_T threhsold to 40 GeV, which helps to suppress PU jets, and observe 39 events in data vs. an MC prediction of 25 ± 5.2 (stat), decreasing the excess from 78% to 58%. In the future this may be improved by explicitly requiring the jets to be consistent with originating from the signal primary vertex.

Based on these studies we currently assess an uncertainty of 80% on the WZ yield.

13

Table 6: Data and Monte Carlo yields passing the WZ preselection.

Sample	ee	$\mu\mu$	eμ	total
WZ	58.9 ± 0.7	82.2 ± 0.8	4.0 ± 0.2	145.1 ± 1.0
$t\bar{t}$	0.6 ± 0.5	4.3 ± 1.5	3.0 ± 1.2	8.0 ± 2.0
$Z + \text{jets}$	0.4 ± 0.4	4.9 ± 4.9	0.0 ± 0.0	5.3 ± 4.9
ZZ	1.4 ± 0.0	2.0 ± 0.0	0.1 ± 0.0	3.5 ± 0.0
WW	0.0 ± 0.0	0.2 ± 0.1	0.2 ± 0.1	0.3 ± 0.1
single top	0.0 ± 0.0	0.0 ± 0.0	0.0 ± 0.0	0.1 ± 0.1
total SM MC	61.3 ± 0.9	93.7 ± 5.2	7.3 ± 1.3	162.3 ± 5.4
data	68	108	14	190

Table 7: Data and Monte Carlo yields passing the WZ preselection and $N_{\text{jets}} > 2$.

| Sample	ee	$\mu\mu$	eμ	total
WZ	9.8 ± 0.3	13.3 ± 0.3	0.6 ± 0.1	23.6 ± 0.4
$t\bar{t}$	0.2 ± 0.2	2.0 ± 0.9	2.2 ± 1.2	4.4 ± 1.5
$Z + \text{jets}$	0.0 ± 0.0	4.9 ± 4.9	0.0 ± 0.0	4.9 ± 4.9
ZZ	0.3 ± 0.0	0.4 ± 0.0	0.0 ± 0.0	0.7 ± 0.0
WW	0.0 ± 0.0	0.0 ± 0.0	0.0 ± 0.0	0.1 ± 0.0
single top	0.0 ± 0.0	0.0 ± 0.0	0.0 ± 0.0	0.0 ± 0.0
total SM MC	10.3 ± 0.3	20.8 ± 5.0	2.8 ± 1.2	33.8 ± 5.2
data	23	32	5	60
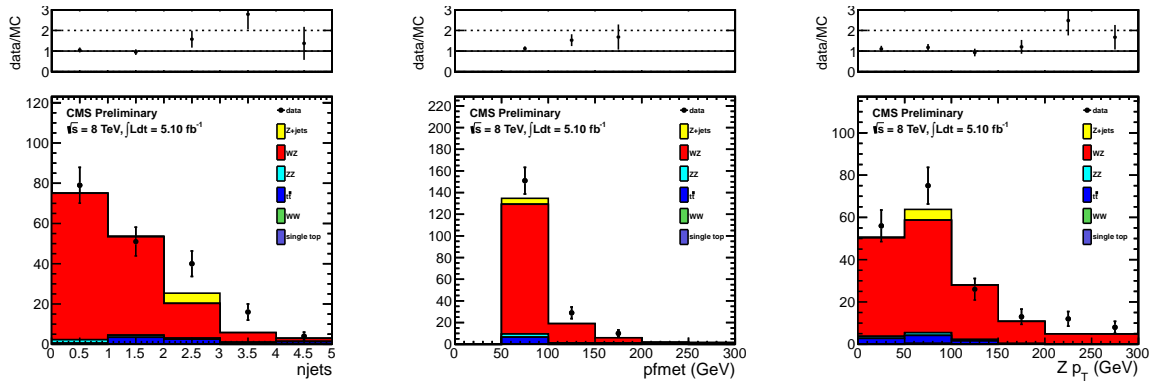
Figure 8: Data vs. MC comparisons for the WZ selection discussed in the text for 5.1 fb^{-1}. The number of jets, missing transverse energy, and Z boson transverse momentum are displayed.

5.3.2 ZZ Validation Studies

274 A pure ZZ sample can be selected in data with the requirements:

275   • Exactly 4 $p_T > 20$ GeV leptons passing analysis identication and isolation requirements,

276   • 2 of the 4 leptons must fall in the Z window 81-101 GeV.

277 The data and MC yields passing the above selection are in Table 8. Again we observe an excess in data with respect
278 to the MC prediction (29 observed vs. 17.3 ± 0.1 (stat) MC predicted). After requiring at least 2 jets, we observe 2
279 events and the MC predicts 1.5 ± 0.1 (stat). However, we have recently discovered that we may be using the wrong
280 (too small) cross section for the ZZ sample, and we are in contact with the MC generator group to determine the
281 correct cross section. Based on this we currently apply an uncertainty of 80% to the ZZ background.

Table 8: Data and Monte Carlo yields for the ZZ preselection.

Sample	ee	$\mu\mu$	eμ	total
ZZ	6.6 ± 0.0	9.9 ± 0.0	0.4 ± 0.0	17.0 ± 0.1
WZ	0.1 ± 0.0	0.2 ± 0.0	0.0 ± 0.0	0.3 ± 0.0
$Z + \text{jets}$	0.0 ± 0.0	0.0 ± 0.0	0.0 ± 0.0	0.0 ± 0.0
$t\bar{t}$	0.0 ± 0.0	0.0 ± 0.0	0.0 ± 0.0	0.0 ± 0.0
WW	0.0 ± 0.0	0.0 ± 0.0	0.0 ± 0.0	0.0 ± 0.0
single top	0.0 ± 0.0	0.0 ± 0.0	0.0 ± 0.0	0.0 ± 0.0
total SM MC	6.7 ± 0.0	10.1 ± 0.1	0.5 ± 0.0	17.3 ± 0.1
data	13	16	0	29
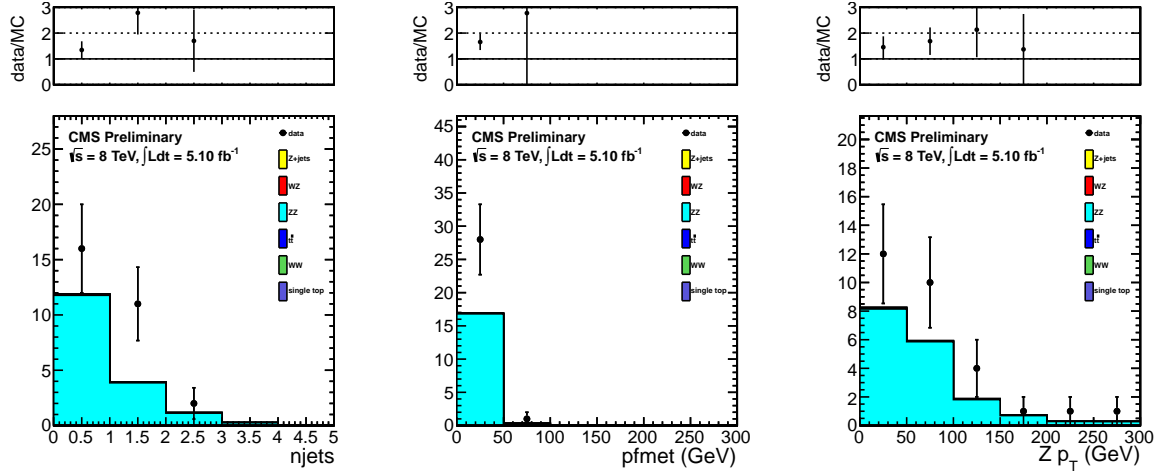
Figure 9: Data vs. MC comparisons for the ZZ selection discussed in the text for 5.1 fb^{-1}. The number of jets,
missing transverse energy, and Z boson transverse momentum are displayed.

₂₈₂ 6 Results

₂₈₃ In this section we provide the results of the inclusive and targeted searches. The observed and predicted E_T^{miss}
₂₈₄ distributions for the inclusive analysis are indicated in Fig. 10. A summary of the results in the signal regions is
₂₈₅ provided in Table 9. In the low E_T^{miss} region ($E_T^{miss} < 100$ GeV) which is dominated by the $Z + \text{jets}$ background,
₂₈₆ the observed yields are in good agreement with the predicted background. This is also the case in the high E_T^{miss}
₂₈₇ region ($E_T^{miss} > 200$ GeV). In the moderate E_T^{miss} region ($100 < E_T^{miss} < 200$ GeV) we observe a slight excess
₂₈₈ in the data with respect to the predicted background. Taking into account the full uncertainty on the background
₂₈₉ prediction, the significance of the excess is about 1.3σ. The separate results for the ee and $\mu\mu$ channels are
₂₉₀ presented in App. A. For this E_T^{miss} region, we find an excess of 1.4σ in the ee channel and 0.7σ in the $\mu\mu$ channel.
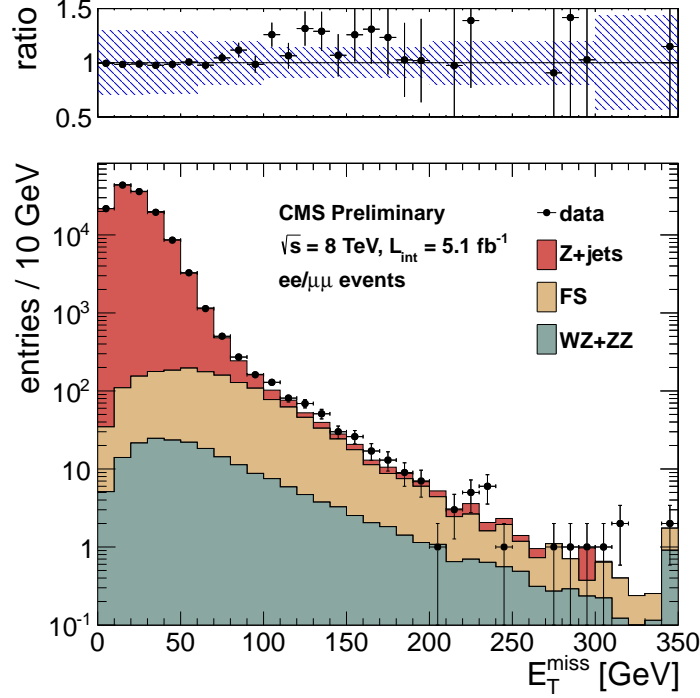

Figure 10: Results of the inclusive analysis. The observed E_T^{miss} distribution (black points) is compared with the sum of the predicted E_T^{miss} distributions from $Z + \text{jets}$, flavor-symmetric backgrounds, and WZ+ZZ backgrounds. The ratio of observed to predicted yields in each bin is indicated. The error bars indicate the statistical uncertainty in the data and the shaded band indicates the total background uncertainty.

Table 9: Summary of results in the inclusive analysis. The total background is the sum of the $Z + \text{jets}$ background predicted from the E_T^{miss} templates method ($Z + \text{jets}$ bkg), the flavor-symmetric background predicted from eμ events (FS bkg), and the WZ and ZZ backgrounds predicted from MC (WZ bkg and ZZ bkg). All uncertainties include both the statistical and systematic components. The Gaussian significance of the deviation between the data and total background is indicated for signal regions with at least 20 observed events.

	$E_T^{miss} > 0$ GeV	$E_T^{miss} > 30$ GeV	$E_T^{miss} > 60$ GeV	$E_T^{miss} > 100$ GeV	$E_T^{miss} > 200$ GeV	$E_T^{miss} > 300$ GeV
$Z + \text{jets}$ bkg	134792 ± 40438	32856 ± 9858	1546 ± 464	68.6 ± 20.8	4.3 ± 1.4	0.0 ± 0.0
FS bkg	1539 ± 239	1281 ± 199	793 ± 123	274 ± 43	13.7 ± 2.5	1.8 ± 1.1
WZ bkg	168.6 ± 134.9	132.5 ± 106.0	71.6 ± 57.3	28.9 ± 23.1	4.2 ± 3.4	0.9 ± 0.7
ZZ bkg	35.6 ± 28.5	31.1 ± 24.9	21.8 ± 17.5	11.9 ± 9.5	2.5 ± 2.0	0.6 ± 0.5
total bkg	136535 ± 40439	34300 ± 9860	2432 ± 484	383 ± 54	24.7 ± 4.9	3.3 ± 1.4
data	134793	33810	2526	456	24	5
significance	-0.0	-0.0	0.2	1.3	-0.1	

The observed and predicted E_T^{miss} distributions for the targeted analysis are indicated in Fig. 11. A summary of the results in the signal regions is provided in Table 10. The observed yields are in good agreement with the predicted background in all signal regions.
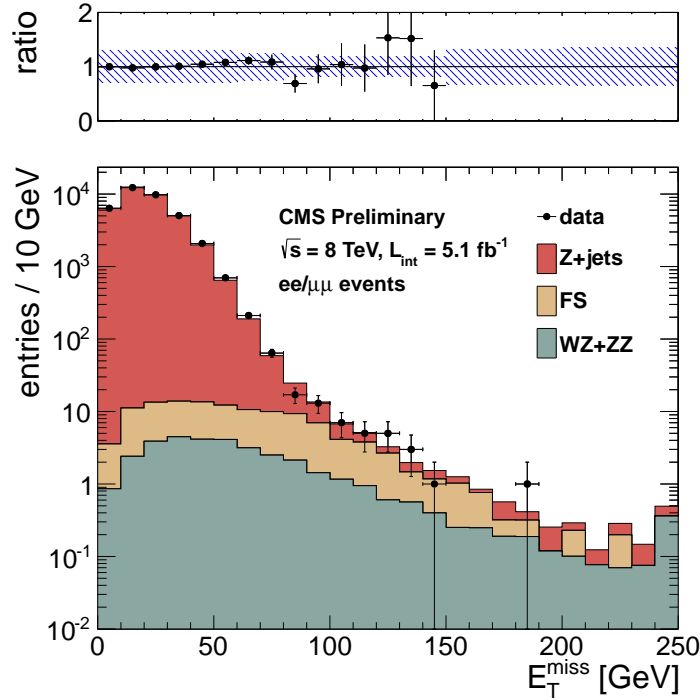

Figure 11: Results of the targeted analysis. The observed E_T^{miss} distribution (black points) is compared with the sum of the predicted E_T^{miss} distributions from $Z + \mathrm{jets}$, flavor-symmetric backgrounds, and WZ+ZZ backgrounds. The ratio of observed to predicted yields in each bin is indicated. The error bars indicate the statistical uncertainty in the data and the shaded band indicates the total background uncertainty.

Table 10: Summary of results in the targeted analysis. The total background is the sum of the $Z + \mathrm{jets}$ background predicted from the E_T^{miss} templates method ($Z + \mathrm{jets}$ bkg), the flavor-symmetric background predicted from eμ events (FS bkg), and the WZ and ZZ backgrounds predicted from MC (WZ bkg and ZZ bkg). All uncertainties include both the statistical and systematic components. The Gaussian significance of the deviation between the data and total background is indicated for signal regions with at least 20 observed events.

	$E_T^{miss} > 0$ GeV	$E_T^{miss} > 30$ GeV	$E_T^{miss} > 60$ GeV	$E_T^{miss} > 80$ GeV	$E_T^{miss} > 100$ GeV	$E_T^{miss} > 150$ GeV	$E_T^{miss} > 200$ GeV
$Z + \mathrm{jets}$ bkg	36487 ± 10947	7856 ± 2357	257 ± 77	28.6 ± 8.7	6.6 ± 2.0	1.2 ± 0.4	0.4 ± 0.1
FS bkg	86.9 ± 14.7	65.9 ± 11.3	39.0 ± 6.8	24.1 ± 4.3	11.3 ± 2.2	1.8 ± 1.1	0.3 ± 0.2
WZ bkg	26.9 ± 21.5	20.9 ± 16.7	10.5 ± 8.4	6.0 ± 4.8	3.4 ± 2.7	0.9 ± 0.7	0.3 ± 0.3
ZZ bkg	7.6 ± 6.1	6.4 ± 5.1	4.1 ± 3.3	2.9 ± 2.3	1.9 ± 1.6	0.8 ± 0.6	0.3 ± 0.3
total bkg	36608 ± 10947	7949 ± 2357	310 ± 78	61.6 ± 11.1	23.3 ± 4.4	4.7 ± 1.5	1.3 ± 0.5
data	36487	8144	327	52	22	1	0
significance	-0.0	0.1	0.2	-0.7	-0.2		

7 Interpretation

The results of this search will be interpreted in the context of simplified model spectra (SMS). For the inclusive analysis, we will use the T5zz model depicted in Fig. 1 (left). For the targeted analysis, we will use the TChiWZ model depicted in Fig. 1 (right), and a GMSB model which produces a signature of $ZZ + E_T^{miss}$.

8 Summary

This note presents a search for BSM physics in final states with leptonically-decaying Z bosons, jets, and E_T^{miss}. Two strategies were pursued. The first is an inclusive approach which targets BSM scenarios with Z bosons produced in the decays of strongly-interacting particles. The second is a targeted approach which focuses on BSM

scenarios where the Z bosons are produced in the decays of weakly-interacting particles. The main backgrounds are estimated with data-driven techniques. No excesses above the SM backgrounds are observed.

References

[1] CMS Collaboration, "Search for physics beyond the standard model in events with a Z boson, jets, and missing transverse energy in pp collisions at $\sqrt{s} = 7$ TeV,", arXiv:1204.3774v1 [hep-ex].

[2] SUS-12-006, paper draft

[3] https://twiki.cern.ch/twiki/bin/viewauth/CMS/EgammaCutBasedIdentification

[4] https://twiki.cern.ch/twiki/bin/viewauth/CMS/EgammaEARhoCorrection

[5] https://twiki.cern.ch/twiki/bin/view/CMSPublic/SWGuideMuonId

[6] M. Chen, AN 2012/237 "Interpretation of the Same-Sign di-leptons with bjets and MET search"

A   Results in the ee and $\mu\mu$ Channels

In this section we provide the results of the inclusive and targeted searches, separately in the ee and $\mu\mu$ channels. The E_T^{miss} distributions in the inclusive analysis for the ee channel are displayed in Fig. 12 and the signal region yields are presented in Table 11. The E_T^{miss} distributions in the inclusive analysis for the $\mu\mu$ channel are displayed in Fig. 13 and the signal region yields are presented in Table 12.
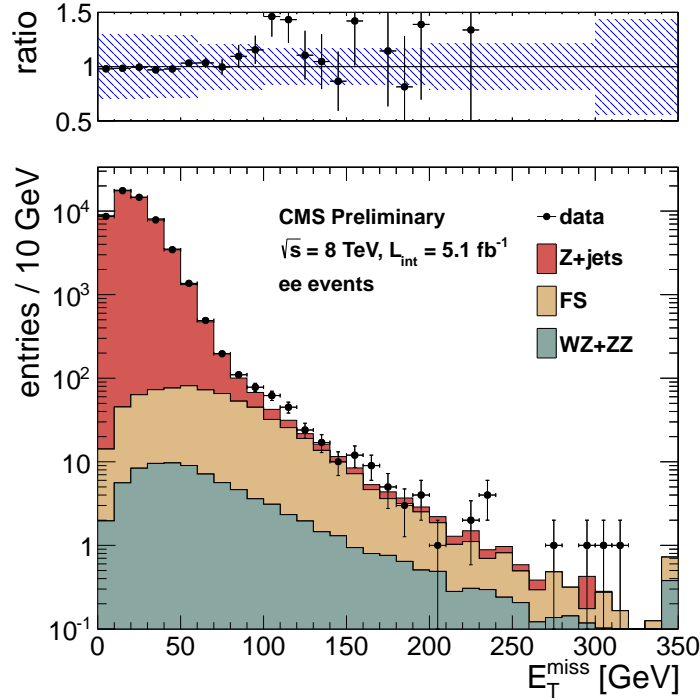
Figure 12: Results of the inclusive analysis in the ee channel. The observed E_T^{miss} distribution (black points) is compared with the sum of the predicted E_T^{miss} distributions from $Z + \text{jets}$, flavor-symmetric backgrounds, and WZ+ZZ backgrounds. The ratio of observed to predicted yields in each bin is indicated. The error bars indicate the statistical uncertainty in the data and the shaded band indicates the total background uncertainty.

Table 11: Summary of results in the inclusive analysis in the ee channel. The total background is the sum of the $Z + \text{jets}$ background predicted from the E_T^{miss} templates method ($Z + \text{jets}$ bkg), the flavor-symmetric background predicted from eμ events (FS bkg), and the WZ and ZZ backgrounds predicted from MC (WZ bkg and ZZ bkg). All uncertainties include both the statistical and systematic components. The Gaussian significance of the deviation between the data and total background is indicated for signal regions with at least 20 observed events.

|	$E_T^{miss} > 0$ GeV	$E_T^{miss} > 30$ GeV	$E_T^{miss} > 60$ GeV	$E_T^{miss} > 100$ GeV	$E_T^{miss} > 200$ GeV	$E_T^{miss} > 300$ GeV
$Z + \text{jets}$ bkg	54427 ± 16334	13306 ± 4000	631 ± 197	28.2 ± 12.7	1.8 ± 0.6	0.0 ± 0.0
FS bkg	637 ± 119	530 ± 99	328 ± 61	113 ± 21	5.7 ± 1.2	0.7 ± 0.5
WZ bkg	67.6 ± 54.1	53.4 ± 42.7	28.9 ± 23.1	11.8 ± 9.4	1.9 ± 1.5	0.4 ± 0.3
ZZ bkg	14.3 ± 11.5	12.6 ± 10.1	8.9 ± 7.1	5.0 ± 4.0	1.1 ± 0.9	0.3 ± 0.2
total bkg	55147 ± 16334	13902 ± 4002	997 ± 208	158 ± 27	10.4 ± 2.2	1.4 ± 0.6
data	54426	13707	1076	202	11	2
significance	-0.0	-0.0	0.4	1.4		
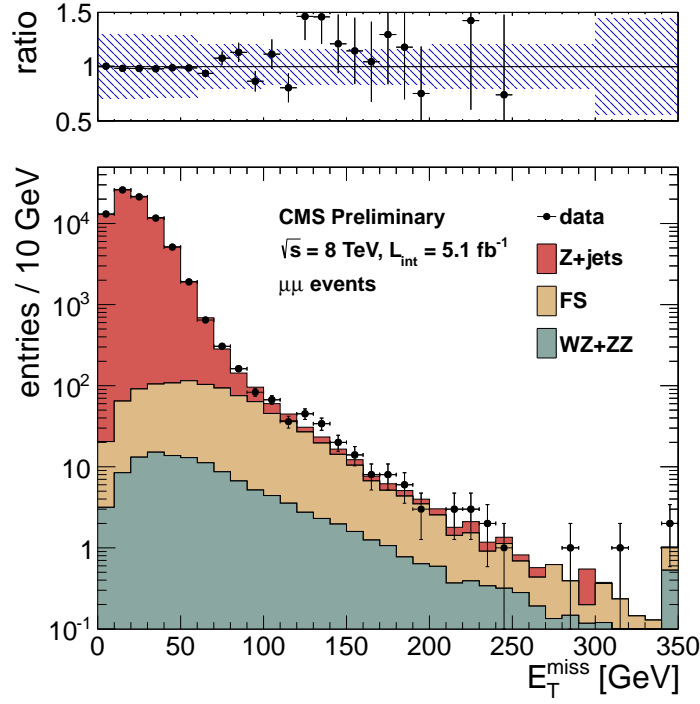
Figure 13: Results of the inclusive analysis in the $\mu\mu$ channel. The observed E_T^{miss} distribution (black points) is compared with the sum of the predicted E_T^{miss} distributions from $Z + \text{jets}$, flavor-symmetric backgrounds, and WZ+ZZ backgrounds. The ratio of observed to predicted yields in each bin is indicated. The error bars indicate the statistical uncertainty in the data and the shaded band indicates the total background uncertainty.

Table 12: Summary of results in the inclusive analysis in the $\mu\mu$ channel. The total background is the sum of the $Z + \text{jets}$ background predicted from the E_T^{miss} templates method ($Z + \text{jets}$ bkg), the flavor-symmetric background predicted from $e\mu$ events (FS bkg), and the WZ and ZZ backgrounds predicted from MC (WZ bkg and ZZ bkg). All uncertainties include both the statistical and systematic components. The Gaussian significance of the deviation between the data and total background is indicated for signal regions with at least 20 observed events.

	$E_T^{miss} > 0$ GeV	$E_T^{miss} > 30$ GeV	$E_T^{miss} > 60$ GeV	$E_T^{miss} > 100$ GeV	$E_T^{miss} > 200$ GeV	$E_T^{miss} > 300$ GeV
$Z + \text{jets}$ bkg	80370 ± 24112	19551 ± 5867	915 ± 276	40.3 ± 13.0	2.6 ± 0.8	0.0 ± 0.0
FS bkg	902 ± 168	750 ± 140	465 ± 87	160 ± 30	8.0 ± 1.7	1.1 ± 0.7
WZ bkg	101.0 ± 80.8	79.0 ± 63.2	42.8 ± 34.2	17.1 ± 13.7	2.3 ± 1.9	0.5 ± 0.4
ZZ bkg	21.3 ± 17.0	18.5 ± 14.8	12.9 ± 10.3	6.9 ± 5.5	1.4 ± 1.1	0.3 ± 0.3
total bkg	81394 ± 24113	20399 ± 5869	1435 ± 292	225 ± 36	14.3 ± 2.9	1.9 ± 0.8
data	80367	20103	1450	254	13	3
significance	-0.0	-0.1	0.1	0.7		

The E_T^{miss} distributions in the targeted analysis for the ee channel are displayed in Fig. 14 and the signal region yields are presented in Table 13. The E_T^{miss} distributions in the inclusive analysis for the $\mu\mu$ channel are displayed in Fig. 15 and the signal region yields are presented in Table 14.
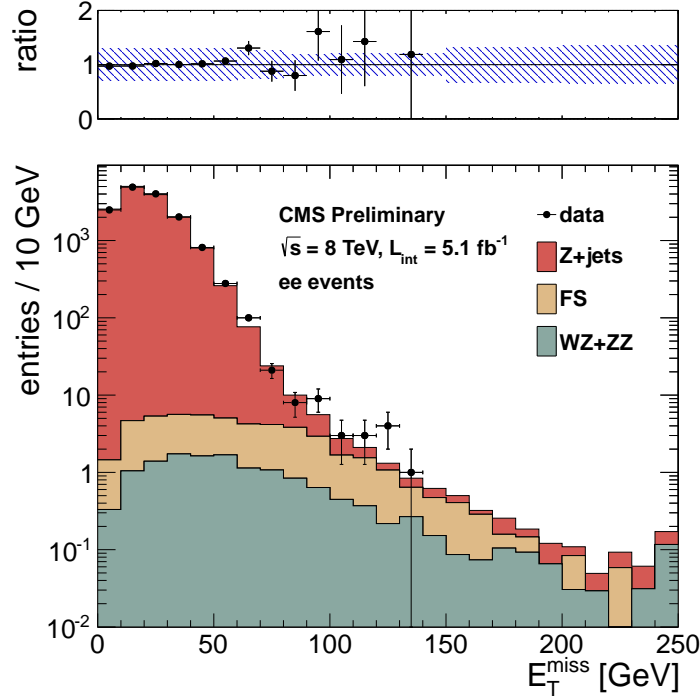

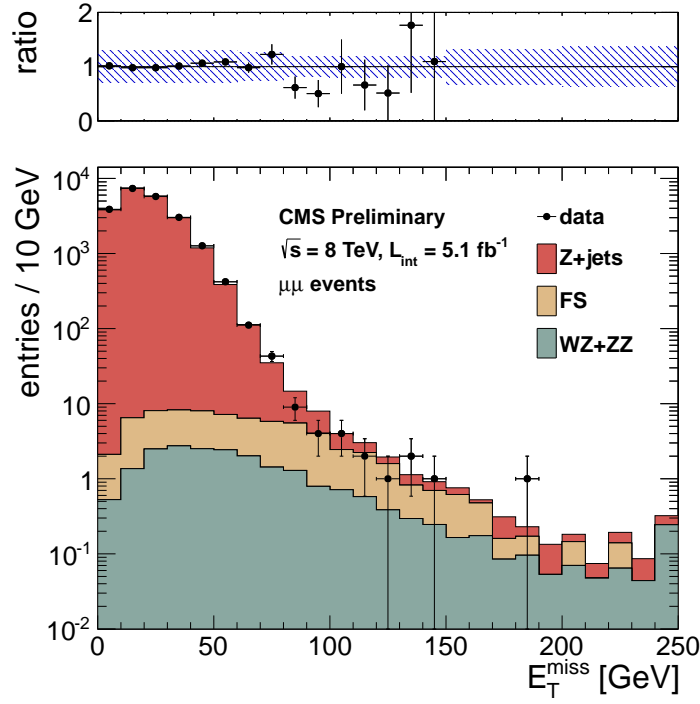
Figure 14: Results of the targeted analysis in the ee channel. The observed E_T^{miss} distribution (black points) is compared with the sum of the predicted E_T^{miss} distributions from Z + jets , flavor-symmetric backgrounds, and WZ+ZZ backgrounds. The ratio of observed to predicted yields in each bin is indicated. The error bars indicate the statistical uncertainty in the data and the shaded band indicates the total background uncertainty.

Table 13: Summary of results in the targeted analysis in the ee channel. The total background is the sum of the Z + jets background predicted from the E_T^{miss} templates method (Z + jets bkg), the flavor-symmetric background predicted from eμ events (FS bkg), and the WZ and ZZ backgrounds predicted from MC (WZ bkg and ZZ bkg). All uncertainties include both the statistical and systematic components. The Gaussian significance of the deviation between the data and total background is indicated for signal regions with at least 20 observed events.

	$E_T^{miss} > 0$ GeV	$E_T^{miss} > 30$ GeV	$E_T^{miss} > 60$ GeV	$E_T^{miss} > 80$ GeV	$E_T^{miss} > 100$ GeV	$E_T^{miss} > 150$ GeV	$E_T^{miss} > 200$ GeV
Z + jets bkg	14647 ± 4395	3159 ± 948	104 ± 32	11.5 ± 3.9	2.7 ± 1.1	0.5 ± 0.2	0.2 ± 0.1
FS bkg	36.0 ± 7.2	27.3 ± 5.5	16.1 ± 3.3	10.0 ± 2.1	4.7 ± 1.0	0.7 ± 0.5	0.1 ± 0.1
WZ bkg	10.6 ± 8.5	8.2 ± 6.6	4.2 ± 3.4	2.4 ± 1.9	1.4 ± 1.1	0.3 ± 0.3	0.1 ± 0.1
ZZ bkg	3.0 ± 2.4	2.6 ± 2.1	1.6 ± 1.3	1.2 ± 0.9	0.7 ± 0.6	0.3 ± 0.2	0.1 ± 0.1
total bkg	14697 ± 4395	3197 ± 948	126 ± 32	25.1 ± 4.9	9.5 ± 1.9	1.9 ± 0.6	0.5 ± 0.2
data	14647	3255	149	28	11	0	0
significance	-0.0	0.1	0.7	0.4			

Figure 15: Results of the targeted analysis in the $\mu\mu$ channel. The observed E_T^{miss} distribution (black points) is compared with the sum of the predicted E_T^{miss} distributions from $Z + jets$, flavor-symmetric backgrounds, and WZ+ZZ backgrounds. The ratio of observed to predicted yields in each bin is indicated. The error bars indicate the statistical uncertainty in the data and the shaded band indicates the total background uncertainty.

Table 14: Summary of results in the targeted analysis in the $\mu\mu$ channel. The total background is the sum of the $Z + jets$ background predicted from the E_T^{miss} templates method ($Z + jets$ bkg), the flavor-symmetric background predicted from $e\mu$ events (FS bkg), and the WZ and ZZ backgrounds predicted from MC (WZ bkg and ZZ bkg). All uncertainties include both the statistical and systematic components. The Gaussian significance of the deviation between the data and total background is indicated for signal regions with at least 20 observed events.

	$E_T^{miss} > 0$ GeV	$E_T^{miss} > 30$ GeV	$E_T^{miss} > 60$ GeV	$E_T^{miss} > 80$ GeV	$E_T^{miss} > 100$ GeV	$E_T^{miss} > 150$ GeV	$E_T^{miss} > 200$ GeV
$Z + jets$ bkg	21840 ± 6552	4697 ± 1409	153 ± 46	17.0 ± 5.3	3.9 ± 1.2	0.7 ± 0.2	0.2 ± 0.1
FS bkg	50.9 ± 10.1	38.6 ± 7.7	22.8 ± 4.6	14.1 ± 2.9	6.6 ± 1.5	1.1 ± 0.6	0.2 ± 0.1
WZ bkg	16.3 ± 13.0	12.7 ± 10.1	6.3 ± 5.0	3.6 ± 2.9	2.1 ± 1.6	0.6 ± 0.5	0.3 ± 0.2
ZZ bkg	4.6 ± 3.7	3.8 ± 3.1	2.5 ± 2.0	1.8 ± 1.4	1.2 ± 1.0	0.5 ± 0.4	0.2 ± 0.2
total bkg	21912 ± 6552	4752 ± 1409	185 ± 47	36.5 ± 6.8	13.8 ± 2.7	2.8 ± 0.9	0.9 ± 0.3
data	21840	4889	178	24	11	1	0
significance	-0.0	0.1	-0.1	-1.5			

B $\quad$ $\mathrm{E}_{\mathrm{T}}^{\mathrm{miss}}$ **Templates from** $\gamma + \mathrm{jets}$ **Sample**
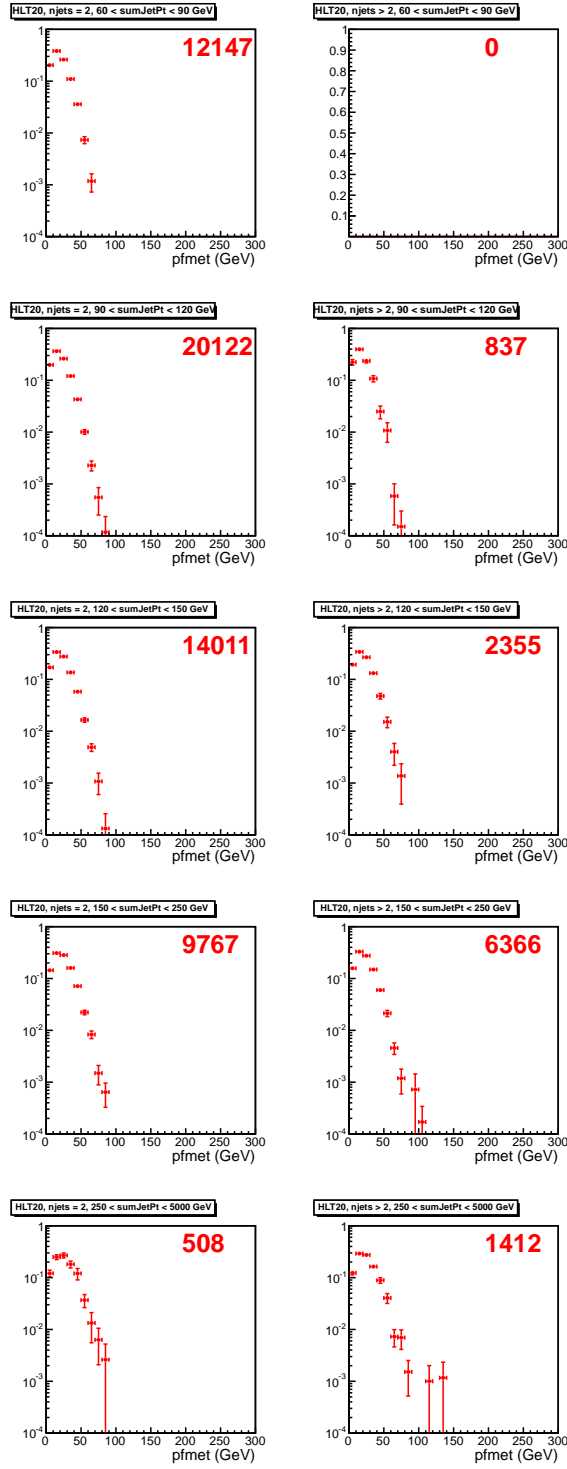

Figure 16: $\mathrm{E}_{\mathrm{T}}^{\mathrm{miss}}$ templates for the inclusive analysis collected with the $p_T > 22$ GeV single photon trigger. The number in red indicates the number of entries in the template.
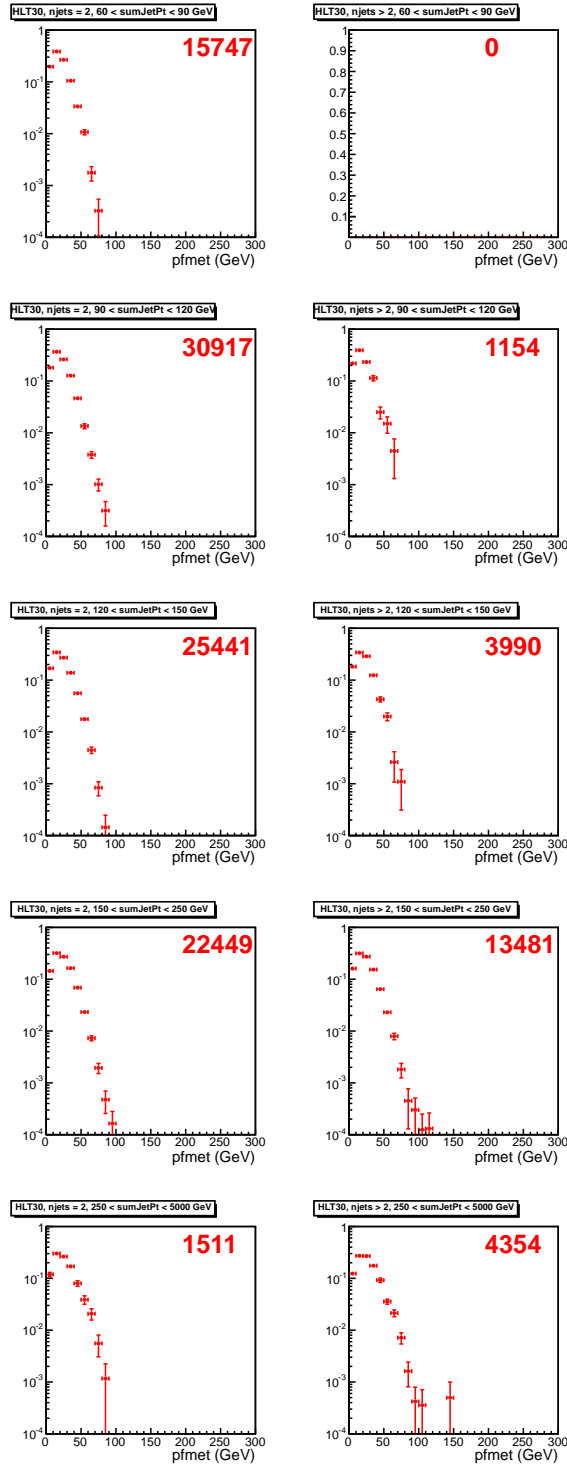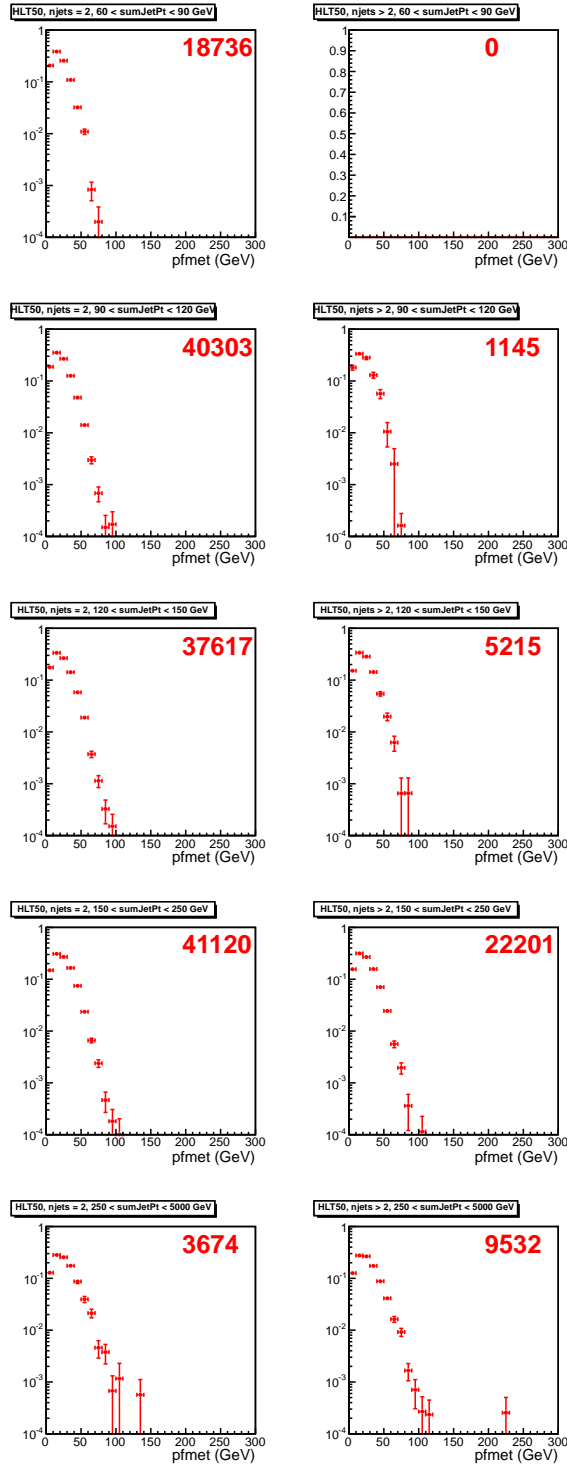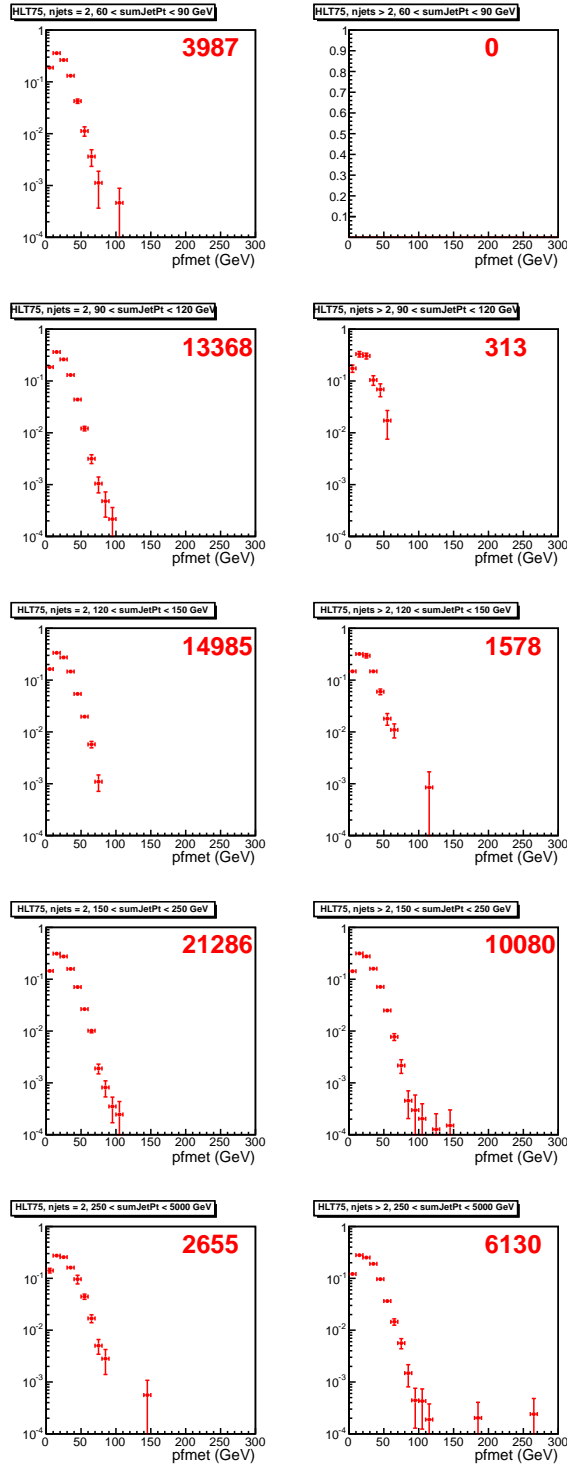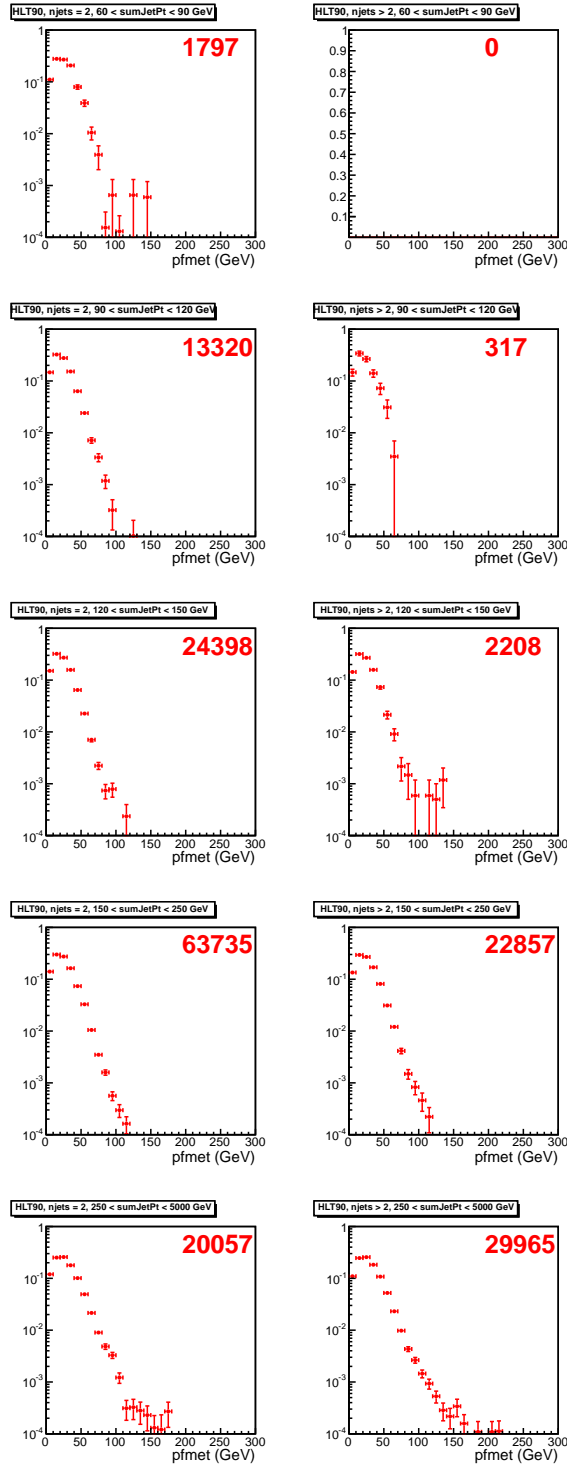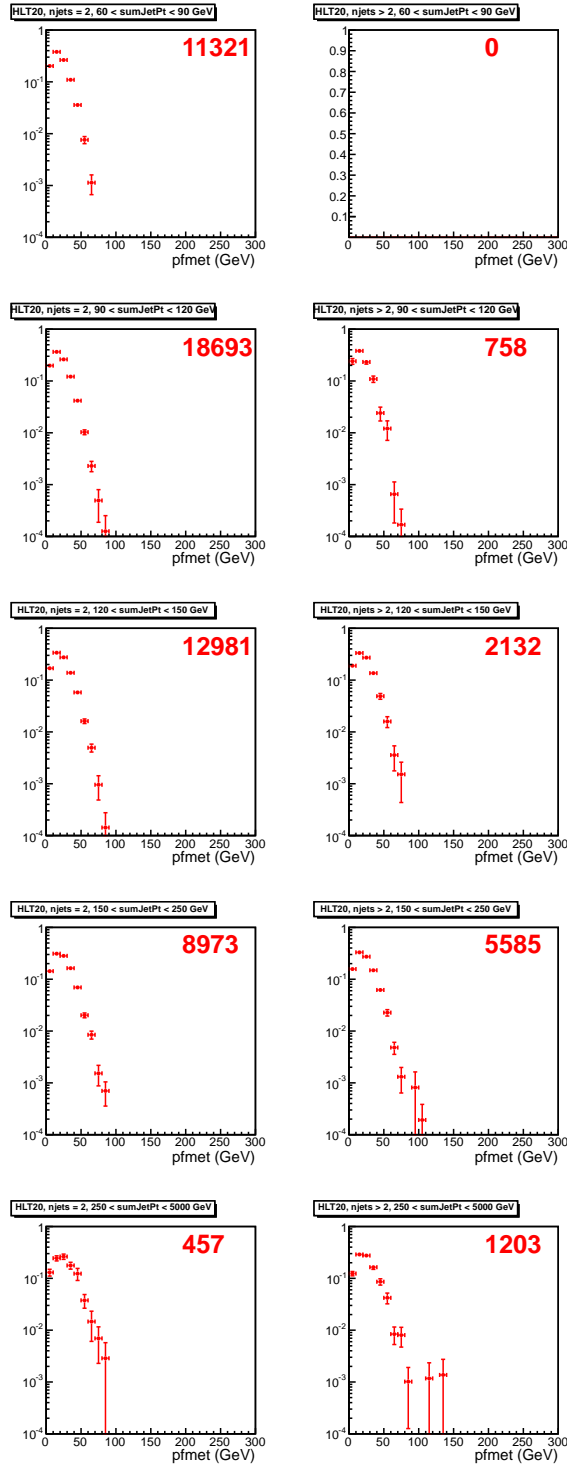
Figure 17: E_T^{miss} templates for the inclusive analysis collected with the $p_T > 36$ GeV single photon trigger. The number in red indicates the number of entries in the template.

Figure 18: E_T^{miss} templates for the inclusive analysis collected with the $p_T > 50$ GeV single photon trigger. The number in red indicates the number of entries in the template.

Figure 19: E_T^{miss} templates for the inclusive analysis collected with the $p_T > 75$ GeV single photon trigger. The number in red indicates the number of entries in the template.
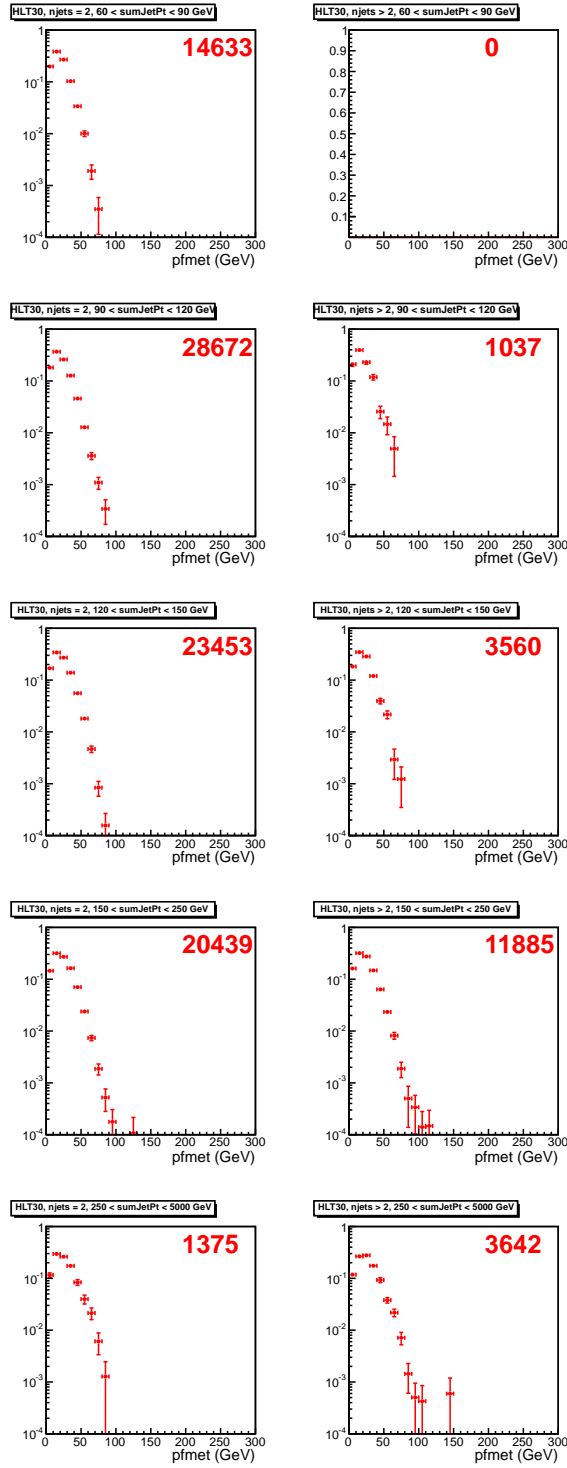
Figure 20: E_T^{miss} templates for the inclusive analysis collected with the $p_T > 90$ GeV single photon trigger. The number in red indicates the number of entries in the template.

Figure 21: E_T^{miss} templates for the targeted analysis collected with the $p_T > 22$ GeV single photon trigger. The number in red indicates the number of entries in the template.

Figure 22: E_T^{miss} templates for the targeted analysis collected with the $p_T > 36$ GeV single photon trigger. The number in red indicates the number of entries in the template.
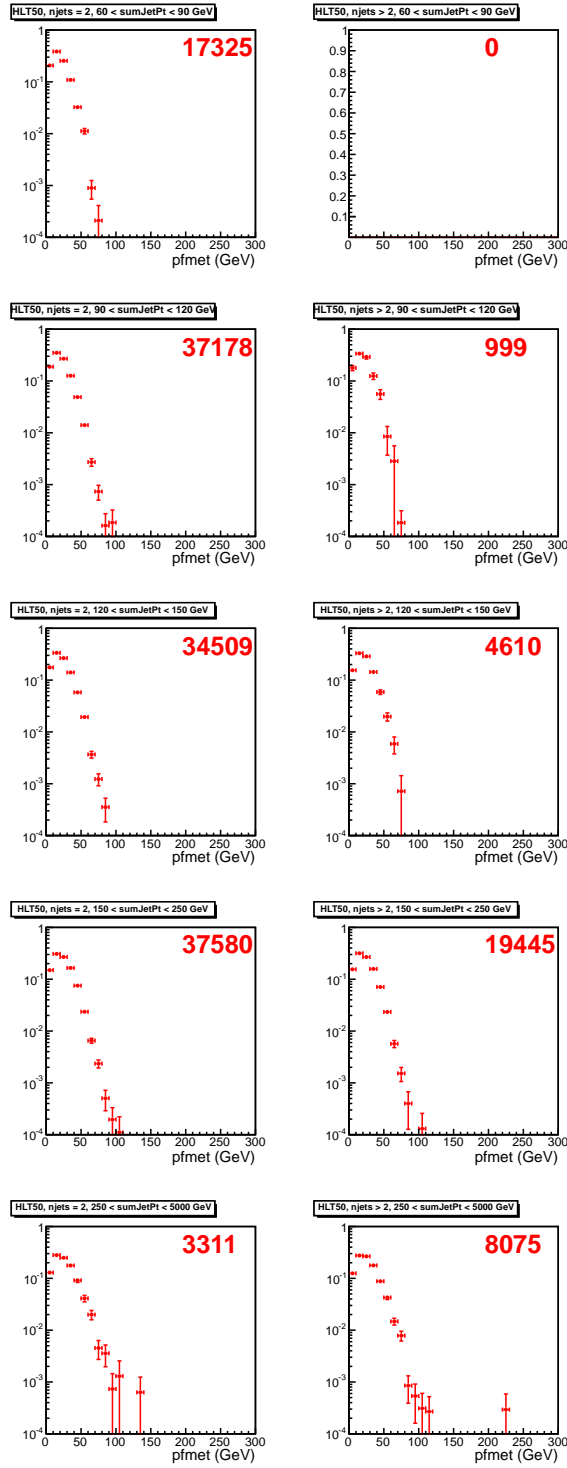
Figure 23: E_T^{miss} templates for the targeted analysis collected with the $p_T > 50$ GeV single photon trigger. The number in red indicates the number of entries in the template.
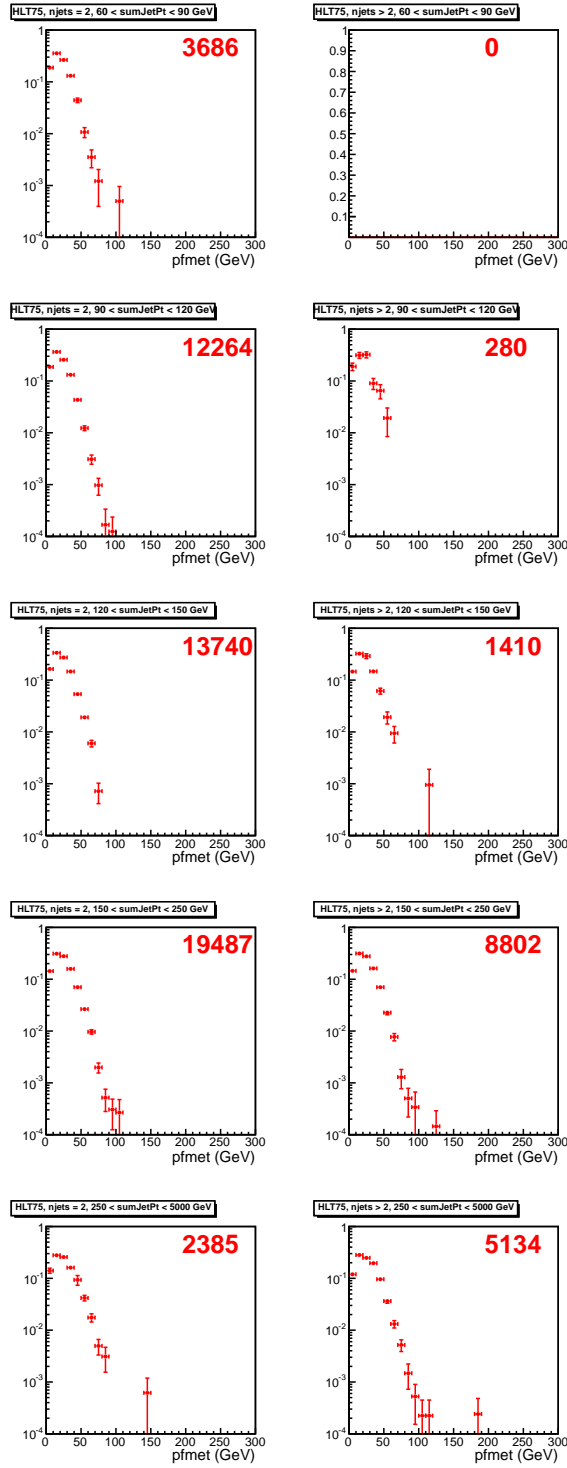
Figure 24: E_T^{miss} templates for the targeted analysis collected with the $p_T > 75$ GeV single photon trigger. The number in red indicates the number of entries in the template.
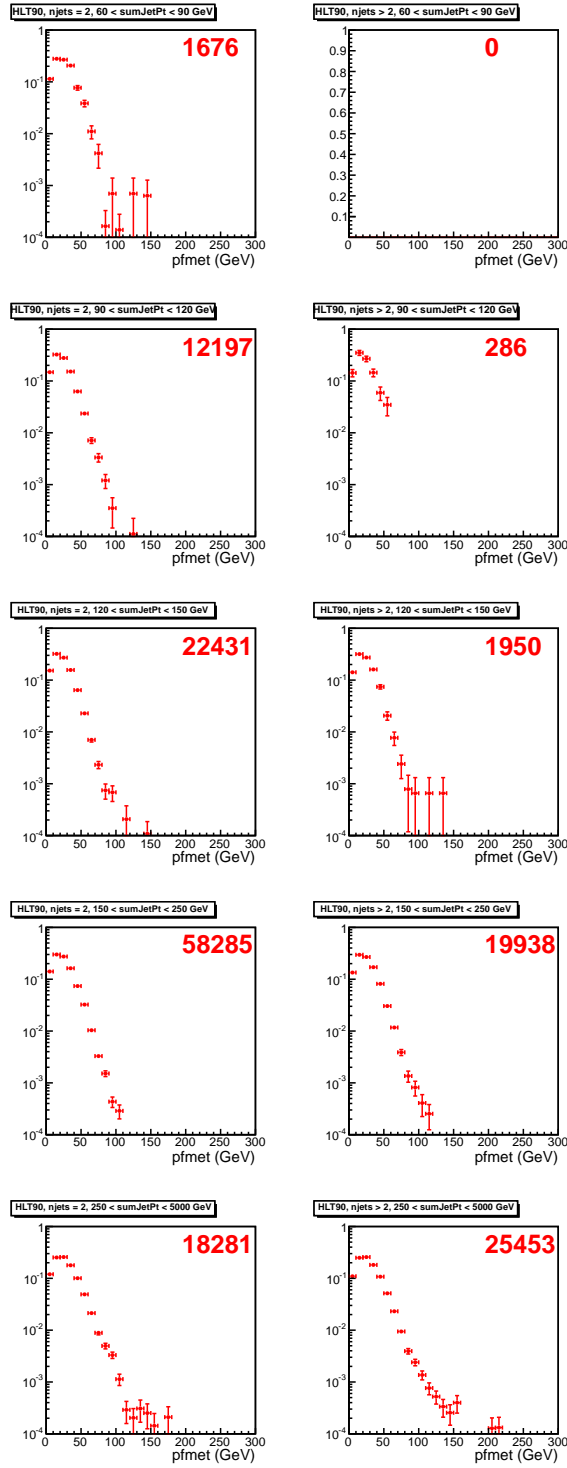
Figure 25: E_T^{miss} templates for the targeted analysis collected with the $p_T > 90$ GeV single photon trigger. The number in red indicates the number of entries in the template.